HURRICANES AND GLOBAL WARMING

Results from Downscaling IPCC AR4 Simulations

BY KERRY EMANUEL, RAGOTH SUNDARARAJAN, AND JOHN WILLIAMS

A new technique for deriving hurricane climatologies from global data, applied to climate models, indicates that global warming should reduce the global frequency of hurricanes, though their intensity may increase in some locations.

Tropical cyclones account for the majority of natural catastrophic losses in the developed world and, next to floods, are the leading cause of death and injury among natural disasters affecting developing countries (UNDP/BCPR 2004). It is thus of some interest to understand how their behavior is affected by climate change, whether natural or anthropogenic.

A range of techniques has been brought to bear on this question. The most straightforward approach is to quantify the response of tropical cyclone activity to past climate change using historical climate and storm records, but this approach is limited by the relatively short length of tropical storm records. In the North Atlantic region, dense ship tracks, islands, and the relatively small size of the basin have led to the creation of an official archive extending back to 1851 (Jarvinen et al. 1984; Landsea et al. 2004), but the detection rate prior to the satellite era remains controversial (Landsea 2007). Routine aircraft reconnaissance of tropical cyclones began shortly after WWII in the North Atlantic and western North Pacific regions, and while it continues to this day over the Atlantic, it was terminated in 1987 over the western North Pacific. These missions undoubtedly improved the detection rate, though it is possible that some storms were still missed. In the active tropical cyclone belts of the eastern North Pacific, and in virtually all of the Southern Hemisphere, high detection rates were not achieved until about 1970, when satellites covered a sufficiently high portion of the globe.

This relatively short and flawed record of tropical cyclone activity has nevertheless led to the detection of significant climatic influences on tropical cyclone activity, most prominently, the influence of El Niño–Southern Oscillation (ENSO) on storms in the North Atlantic (Gray 1984; Bove et al. 1998; Pielke and Landsea 1999; Elsner et al. 2001) and western North Pacific (Chan 1985). Variations on time scales

AFFILIATIONS: EMANUEL, SUNDARARAJAN, AND WILLIAMS—Program in Atmospheres, Oceans, and Climate, Massachusetts Institute of Technology, Cambridge, Massachusetts
CORRESPONDING AUTHOR: Kerry Emanuel, Room 54-1620, MIT, 77 Massachusetts Ave., Cambridge, MA 02139
E-mail: emanuel@texmex.mit.edu

The abstract for this article can be found in this issue, following the table of contents.
DOI:10.1175/BAMS-89-3-xxx

In final form 29 October 2007

of several decades have also been discussed, with early work attributing such variations to natural climate fluctuations, such as the Atlantic Multi-Decadal Oscillation (Goldenberg et al. 2001) and the Pacific decadal oscillation (Chan and Shi 1996). The subsequent attribution of decadal variability and trends to radiatively forced climate change by Emanuel (2005a) and Webster et al. (2005) led to a vigorous debate and reexamination of the quality of the tropical cyclone record (Emanuel 2005b; Landsea 2005; Chan 2006; Landsea et al. 2006; Chang and Guo 2007; Kossin et al. 2007; Landsea 2007), while the sources of the trends and variability continue to be debated (Curry et al. 2006; Hoyos et al. 2006; Santer et al. 2006; Emanuel 2007; Mann et al. 2007).

Another approach to the problem is to extend the tropical cyclone record back into prehistory using proxies for storm activity detected in the geological record, an endeavor known as paleotempestology. Proxies used so far include storm-driven overwash deposits in near-shore lakes and marshes (Liu and Fearn 1993; Donnelly and Woodruff 2007), oxygen isotopic anomalies recorded in speleothems (Malmquist 1997; Frappier et al. 2007) and tree rings (Miller et al. 2006), and storm-driven beach deposits (Nott 2003). Reconstructions of coastal tropical cyclone activity, some of which now extend over thousands of years, are beginning to reveal patterns of variability on decadal-to-centennial time scales (Liu and Fearn 1993; Donnelly and Woodruff 2007). At present, such techniques are limited to coastal regions.

Basic theory has been used to predict the dependence of hurricane intensity (as measured by maximum wind speeds or minimum surface pressures) on climate (Emanuel 1987), but there is at present very little theoretical guidance pertaining to the frequency or duration of events. Potential intensity theory (Emanuel 1986; Bister and Emanuel 1998) has been widely interpreted as predicting a particular dependence of tropical cyclone wind speeds on sea surface temperature (Landsea 2005), though in reality the predicted dependence is on the air–sea thermodynamic disequilibrium and lower-stratospheric temperature; the former of which can be shown to depend mostly on the net surface radiative flux and the average near-surface wind speed (Emanuel 2007). The robust 10% increase in summertime potential intensity over the tropical North Atlantic since about 1990 has been shown to depend on increasing net surface radiative flux, cooling lower-stratospheric temperature, and decreasing surface wind speeds (Emanuel 2007). Sea surface temperature is merely a cofactor. Application of potential intensity theory to the output of a global climate model by Emanuel (1987) showed a significant increase of potential intensity in a double-CO_2 climate.

The horizontal resolution of the current generation of global climate models is insufficient to simulate the complex inner core of intense tropical cyclones; the highest resolution achieved to date has a horizontal grid spacing of 20 km (Oouchi et al. 2006), whereas numerical convergence tests using mesoscale models suggest that grid spacing of the order of 1 km may be required (Chen et al. 2007). Nevertheless, many global models produce reasonable facsimiles of tropical cyclones, and many studies have documented the effects of climate change on these simulated disturbances (Bengtsson et al. 1996; Sugi et al. 2002; Oouchi et al. 2006; Yoshimura et al. 2006; Bengtsson et al. 2007). While there is a wide variation in the results of these studies, there is a tendency toward decreasing frequency and increasing intensity and precipitation of tropical cyclones as the climate warms (Bengtsson et al. 2007).

Another way to use global models to assess future tropical cyclone activity is to identify changes in large-scale environmental factors that are known to affect storm activity. For example, a recent study by Vecchi and Soden (2007) showed that a consensus of global climate models predicts increasing wind shear over the North Atlantic with warming. This would tend to inhibit tropical cyclone activity, all other things being equal.

The limitations of the low resolution of the GCMs can be circumvented by embedding in them high-resolution regional models, an approach that was pioneered by Knutson et al. (1998) and Knutson and Tuleya (2004). In this method, the GCM supplies boundary and initial conditions to the regional model, which produces its own climatology of tropical cyclones. This approach has been applied so far to idealized climate change scenarios (Knutson et al. 1998; Knutson and Tuleya 2004), to the climate of the late twentieth century (Knutson et al. 2007), and most recently to future climates affected by global warming (T. Knutson 2007, personal communication). This last study drove a regional model of the tropical North Atlantic with a large-scale environment created by averaging the output of 18 GCMs used for the most recent report of the Intergovernmental Panel on Climate Change (IPCC). The results are notable in that they predict decreasing storm activity over the North Atlantic, perhaps as a consequence of increased vertical wind shear (Vecchi and Soden 2007), which is a circumstance widely recognized as inhibiting cyclone activity.

These methods of downscaling are producing useful insights into the dependence of tropical cyclone activity on climate. At the present time, they are still limited in horizontal resolution, using grid spacing of around 18 km, and they are expensive to conduct, so that only a limited number of simulations can be performed. For this reason, it is desirable to supplement these studies with methods that use simpler embedded models that can be run a large number of times so as to produce statistically robust estimates of the probability distributions of storms in different climates.

The method pursued in this paper is an extension of that described by Emanuel et al. (2006) and Emanuel (2006). Here we provide a brief overview of the technique; the reader is referred to Emanuel et al. (2006) and their online supplement for a complete description. Broadly, this approach uses both thermodynamic and kinematic statistics derived from global model or reanalysis gridded data to produce large ($\sim 10^3$–10^4) numbers of synthetic tropical cyclones, and these statistics are then used to characterize the tropical cyclone climatology of the given global climate. The synthetic tropical cyclones are produced in the following three steps:

1) *Genesis.* In previous implementations, tracks are initiated by randomly drawing from a space–time genesis probability distribution based strictly on historical tropical cyclone data. In the "Genesis by random seeding" section of this paper we describe a new technique based on random seeding, which uses no historical data.
2) *Tracks.* We developed two independent track models, the first of which represents each track as a Markov chain driven by historical tropical cyclone track statistics as a function of location and time, while the second uses a "beta and advection" model to predict storm tracks using only the large-scale background wind fields and a correction to account for drift induced by the storm's advection of the planetary vorticity field. Here we employ the second method, because we wish to predict tracks in future climates as well as the present. The beta-and-advection model uses synthetic wind time series of 850 and 250 hPa, represented as Fourier series of random phase constrained to have the monthly means, variances, and covariances calculated using daily data from reanalyses or global models, and to have a geostrophic turbulence power-law distribution of kinetic energy.
3) *Intensity.* The wind field of each storm is predicted using a deterministic, coupled air–sea model, the "Coupled Hurricane Intensity Prediction System" ("CHIPS"). The great advantage of this model is that it is phrased in angular momentum coordinates, permitting a very high radial resolution of the critical inner-core region using only a limited number of radial nodes. This model has been optimized over the past 8 yr to produce skillful, real-time hurricane intensity forecasts. With one exception, noted in the "Genesis by random seeding" section below, we use the same version of this model that we use for real-time operational prediction of tropical cyclone intensity (Emanuel et al. 2004). Inputs to this model include the global model's thermodynamic state and wind shear derived from the global model's wind statistics, as described in detail in Emanuel et al. (2006). We also allow for variable midtropospheric temperature and relative humidity, assigning the global model's monthly mean entropy of 600 hPa to the CHIP model's midtropospheric entropy variable. While the thermodynamic state also includes the global model's predicted sea surface temperature, the upper-ocean thermal structure (mixed layer depth and sub–mixed layer thermal stratification) is taken from present climatology, owing to our lack of confidence in such quantities produced by current GCMs. The initialization of this model differs, however, from previous implementations, as described in "Genesis by random seeding." This intensity model is computationally efficient, making very large numbers of simulations feasible.

Aside from genesis, the method described above is independent of historical tropical cyclone data. To apply it to future climates as simulated using global models, it is highly desirable to relate the genesis probability distribution to the actual climate state, rather than to rely on historical distributions. A new technique for doing this is described in the following section, and tests of the technique against observed spatial, seasonal, and interannual variability are presented therein. This is followed by an application to future climates simulated by IPCC Fourth Assessment Report (AR4) models, as described in the "Application to global climate models" section, and a discussion of the results thereafter. A summary concludes the paper.

GENESIS BY RANDOM SEEDING. In the traditional application of the synthetic track technique, storms are initiated at points drawn from a histori-

cally based genesis probability density function, and, in the intensity model, are initiated with a warm-core vortex with peak winds of 17 m s^{-1} (35 kt). Because historically, real tropical cyclones develop at places and times that are favorable for genesis, most of the storms initialized at this amplitude develop to some degree.

As an alternative to this procedure, we initiate tracks at points that are randomly distributed in space and time, but with warm-core vortices that have peak wind speeds of only 12 m s^{-1} (25 kt) and almost no midlevel humidity anomaly in their cores; this causes them to decay initially (Emanuel 1989). These random "seeds" are planted everywhere and at all times, regardless of latitude, SST, season, or other factors, except that storms are not allowed to form equatorward of 2° latitude. These seed vortices track according to the beta-and-advection model, and their intensity is predicted in the usual way using the CHIPS model. The seeds are not considered to form tropical cyclones unless they develop winds of at least 21 m s^{-1} (40 kt). In practice, the great majority of seeds fail to develop by this criterion, succumbing to small potential intensity, large wind shear, or low midtropospheric entropy, and decaying rapidly after initiation.

Notably absent from this technique is any account of the statistics of potential initiating disturbances, such as easterly waves, or the empirical role of large-scale, low-level vorticity in genesis (Gray 1979; Emanuel and Nolan 2004; Camargo et al. 2007). Random seeding assumes, in essence, that the probability of a suitable initiating disturbance is uniform in both space and time. As a variation on random seeding, we therefore experimented with weighting the probability of genesis by various functions of the low-level (850 hPa) vorticity. Slightly improved results are obtained by weighting the genesis probability by the product of the Coriolis parameter and the 850-hPa relative vorticity, not allowing the weighting factor to be negative. We shall refer to this as "vorticity weighting." In no case was genesis observed when the local potential intensity was less than 40 m s^{-1}; thus, to save computing time, we do not seed over land or elsewhere when the potential intensity is less than this value.

The CHIPS model uses a parameterization of the deleterious effect of environmental wind shear on tropical cyclones, developed empirically over years of refining the model's real-time predictions of storm intensity. Real-time predictions are made only for developed storms with maximum wind speeds of at least 17 m s^{-1}, so it is not clear that the same parameterization is optimum for determining the survival in shear of seed disturbances whose initial intensities are only 12 m s^{-1}. At the suggestion of an anonymous reviewer, we modified the shear parameterization in CHIPS in order to make the weaker storms more susceptible to shear. The CHIPS shear parameterization (see Emanuel et al. 2006) has multiplicative factors involving the model's nondimensional maximum wind speed and convective updraft mass flux; here we place lower bounds on these two quantities as they appear in the parameterization. This increases the susceptibility to shear of the weaker disturbances, while leaving shear effects on strong storms unaltered. These lower bounds were loosely adjusted to optimize predictions of seasonal and interannual variability of storms in the current climate. Implementing this adjustment made a small, but noticeable, improvement in the statistics described below.

Figures 1a,b compare the empirical genesis distribution, based on 2,000 events in each of five basins,[1] to the observed distribution from 1690 best-track events, in both cases for storms that go on to attain peak winds of at least 45 kt. The synthetic technique uses reanalysis data from 1980 to 2005, and the best-track genesis points are from the same period. For the present purpose, genesis is defined for the synthetic events as the first point at which the maximum winds exceed 30 kt. In order not to mask regions of infrequent events, the charts plot the logarithm of 1 + the number of points per 2.5° latitude–longitude area, and the absolute rate of genesis of the synthetic events has been calibrated to yield the correct global frequency. The frequencies of best-track and synthetic events are compared for each basin in Fig. 1c.

In general, there are too few events in the Atlantic and eastern North Pacific relative to the rest of the world. The synthetic distribution is weighted too far west in the main development region (MDR) of the Atlantic, between Africa and the Caribbean, and does not have a secondary maximum of activity off the U.S. southeast coast. The local genesis maximum in the Caribbean is well to the southeast of the observed maximum. In the western North Pacific, the simulated storms broadly have the correct distribution, but the genesis region extends too far east and is located too far south in the South China Sea. In the Southern Hemisphere, the synthetic distribution is not far from that observed, but there are too many genesis events

[1] Here the basins are defined as the North Atlantic, the North Pacific east of 160°W, the North Pacific west of 160°W, the northern Indian Ocean, and all of the Southern Hemisphere.

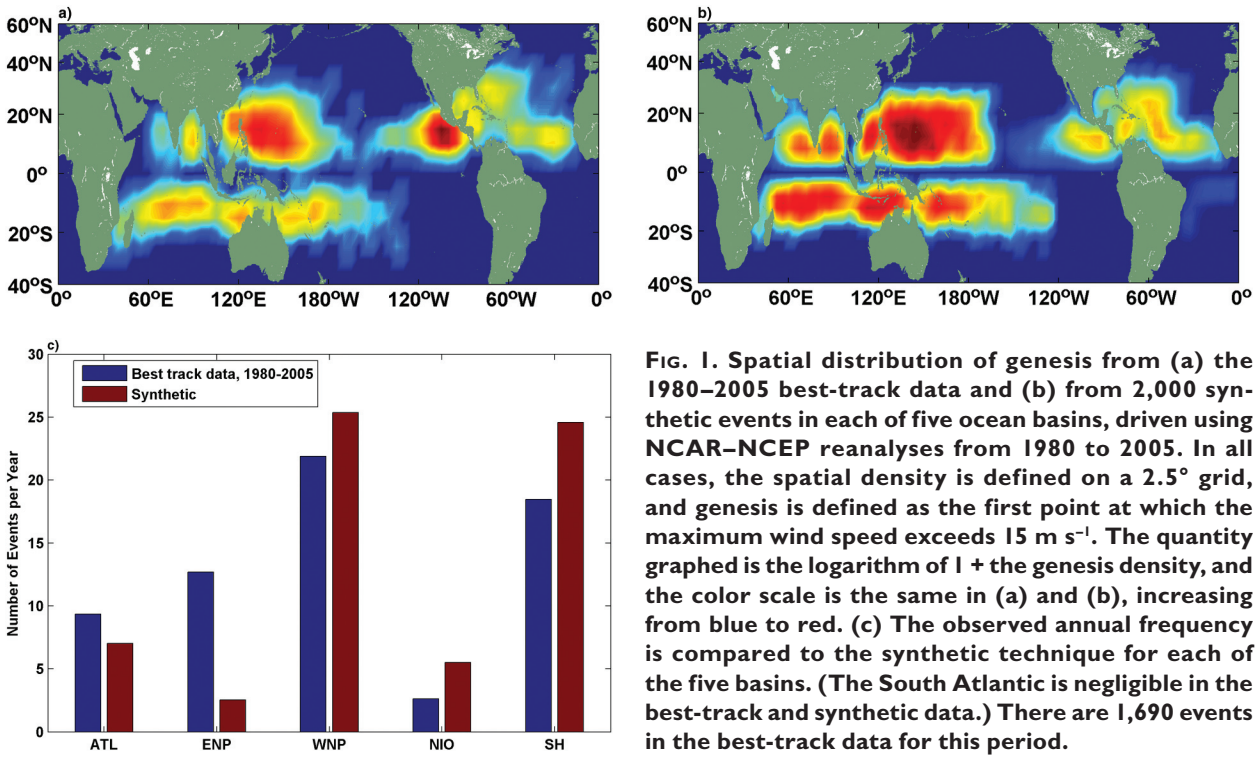

Fig. 1. Spatial distribution of genesis from (a) the 1980–2005 best-track data and (b) from 2,000 synthetic events in each of five ocean basins, driven using NCAR–NCEP reanalyses from 1980 to 2005. In all cases, the spatial density is defined on a 2.5° grid, and genesis is defined as the first point at which the maximum wind speed exceeds 15 m s^{-1}. The quantity graphed is the logarithm of 1 + the genesis density, and the color scale is the same in (a) and (b), increasing from blue to red. (c) The observed annual frequency is compared to the synthetic technique for each of the five basins. (The South Atlantic is negligible in the best-track and synthetic data.) There are 1,690 events in the best-track data for this period.

in the region north of Madagascar. Note that there are a few events in the South Atlantic; the predicted frequency of events in that basin is about (7 yr)$^{-1}$.

In comparing the synthetic to the observed spatial distributions shown in Fig. 1, bear in mind that some of the discrepancies may result from sampling, because there are more than 6 times the number of synthetic events as there are best-track storms. Some of the discrepancies may arise from not accounting for the amplitude and frequency of potential initiating disturbances in this technique; for example, in the Atlantic, African easterly waves and quasi-baroclinic disturbances off the southeast U.S. coast may produce genesis maxima that are not captured here.

The annual cycle of genesis by month is shown in Fig. 2 for each of the five basins, and is compared to the best-track data. To focus on the quality of the annual-cycle per se, we have normalized the annual count in each basin to be equal to the observed count for the period of 1980–2005 in this figure. To estimate the closeness of fit to the data, we create 100 subsamples of the synthetic tracks, each with the same total number of tracks as contained in the best-track data for the given period of time. The confidence limits shown in Fig. 2 represent limits within which 90% of the subsamples are contained. Genesis by random seeding produces an annual cycle very close to that of nature, although there are some interesting discrepancies, particularly in the eastern North Pacific, where the synthetic technique also predicts too few events (Fig. 1c), and in the north Indian Ocean, where too many storms are predicted. In particular, the seasonal cycle in the eastern North Pacific peaks too soon compared to observations, and while the double peak in the north Indian Ocean is reproduced by the random seeding technique, its amplitude is too small, though the sample of observed events is rather small in this case.

Another test of the validity of the random seeding approach is its ability to distinguish between quiet and active periods. An example of particular interest is the well-known modulation of Atlantic tropical cyclone activity by ENSO (Gray 1984; Bove et al. 1998; Pielke and Landsea 1999; Elsner et al. 2001). In particular, El Niño is observed to suppress tropical cyclones in the Atlantic. Figure 3 compares the exceedence frequencies of Atlantic tropical cyclones as function of their lifetime peak wind speed as measured during El Niño and La Niña years, as defined by Pielke and Landsea (1999).[2] Because of the relatively small number of years in each category,

[2] For the present purpose, we lump "weak" and "strong" events into a single category. The index for a particular winter is held to be pertinent to the previous Atlantic hurricane season, and we extended the Pielke and Landsea results by adding 2002 and 2004 to El Niño years, and 1998 and 2000 to La Niña years.

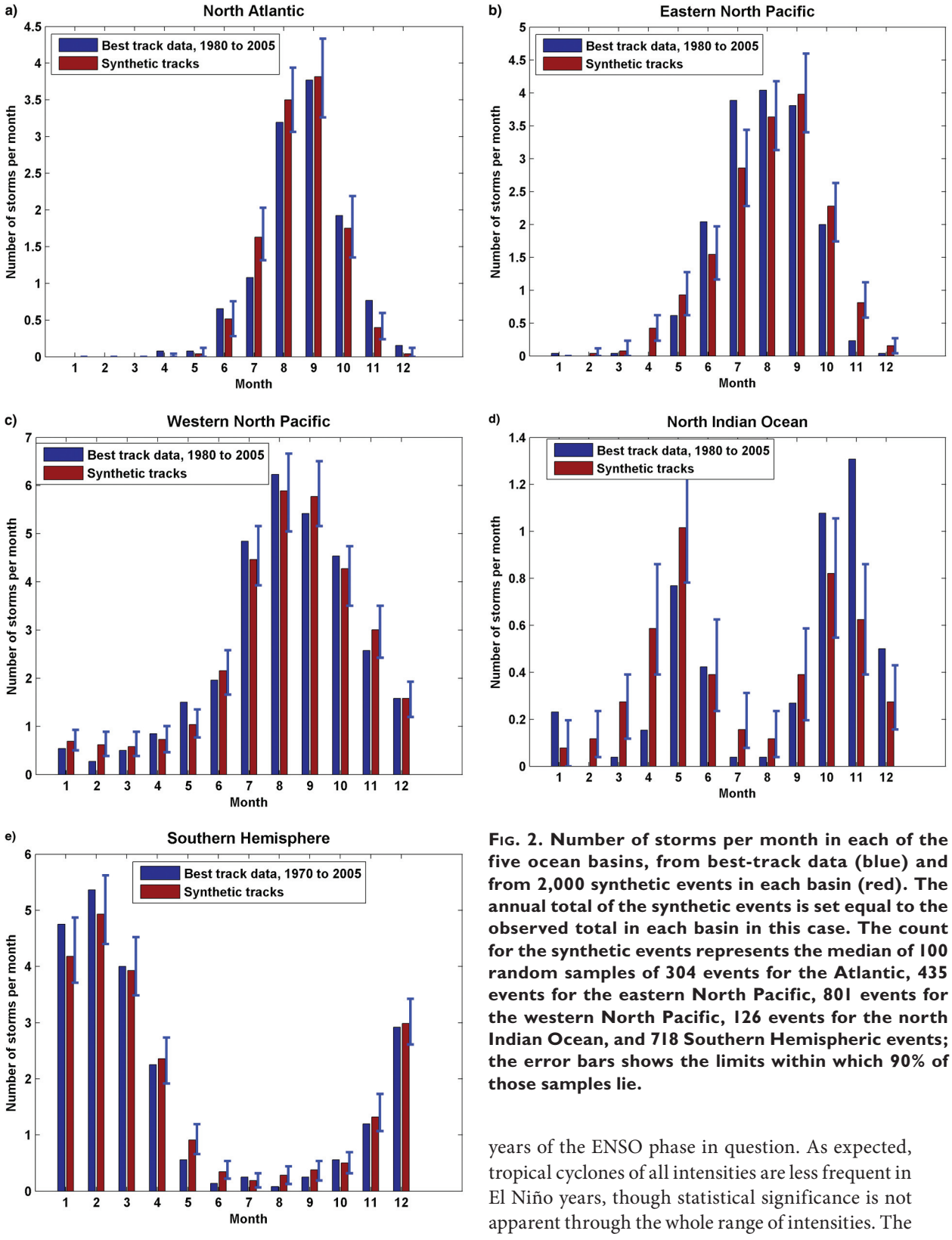

FIG. 2. Number of storms per month in each of the five ocean basins, from best-track data (blue) and from 2,000 synthetic events in each basin (red). The annual total of the synthetic events is set equal to the observed total in each basin in this case. The count for the synthetic events represents the median of 100 random samples of 304 events for the Atlantic, 435 events for the eastern North Pacific, 801 events for the western North Pacific, 126 events for the north Indian Ocean, and 718 Southern Hemispheric events; the error bars shows the limits within which 90% of those samples lie.

we use the full reanalysis period of 1949–2004, and 2,000 synthetic events were run for each ENSO phase, using reanalysis data accumulated over only those years of the ENSO phase in question. As expected, tropical cyclones of all intensities are less frequent in El Niño years, though statistical significance is not apparent through the whole range of intensities. The difference between El Niño and La Niña is not quite as great among the synthetic events as is evident in the observations. To capture enough years in each phase to lend better statistical significance to the

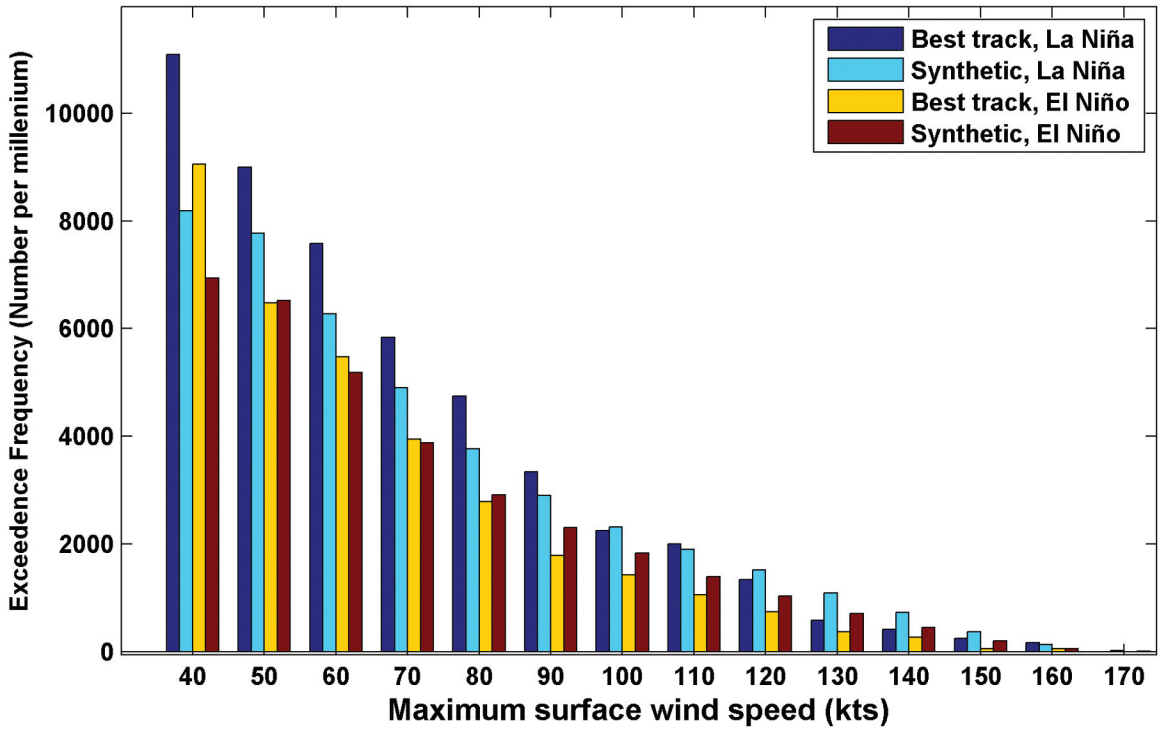

Fig. 3. Exceedence frequency distributions by intensity for North Atlantic storms for La Niña years (dark and light blue bars), and El Niño years (yellow and red bars). In each pair of bars, the best-track data pertain to the left member, and the synthetic data to the right. Data from the two phases of ENSO during the period 1949–2004 are used for both the best-track and reanalysis data.

analysis, it was necessary to use almost the entire 56-yr period of the National Centers for Environmental Prediction–National Center for Atmospheric Research (NCEP–NCAR) reanalysis, and it is well known that there are biases in the reanalysis in the earlier part of this period.

One further test that avoids the use of reanalysis data from early in the record is the comparison each year of the best-track data from 1980 to 2006 with synthetic storms produced using data from each year of the reanalysis in this same time interval.[3] We do this with some reservations, because the wind covariance matrix used to synthesize winds for the track model and for wind shear used as input to the intensity model will be based on only 30 or 31 daily departures from the monthly averages. Nevertheless, if there is any skill in hindcasting tropical cyclone activity, it should be based on the deterministic part of the method, which involves the monthly mean reanalysis data, rather than the random components based on the covariances. To produce this time series, we run 200 synthetic events for each year.

Figure 4a compares the time series of the annual frequency of North Atlantic events from 1980 to 2006 with the observed annual frequency, based on best-track data, and with the annual frequency of events produced in a single simulation with a regional model of the tropical Atlantic driven by boundary conditions supplied from the same NCEP–NCAR reanalysis as is used here, as reported in Knutson et al. (2007). Only storms that occurred in the months of August–October are included in this series, and the Knutson et al. results are based on their single model 2 run. The results here are statistically indistinguishable from those of Knutson et al.; the synthetic method used here explains about the same amount of the observed variance as that of Knutson et al., with a slightly lower root-mean-square error and with a mean trend of 0.19 yr^{-1}, compared to the 0.21 yr^{-1} in Knutson et al. Likewise, the power dissipation by tropical cyclones in both the synthetic method and the Knutson et al. method increases by about 200% over the period, with correlation coefficients between the observed and simulated power dissipation time series of around 0.7 in both cases.

Vitart et al. (2007) attempted to forecast and reforecast Atlantic tropical cyclone activity over the period of 1993–2006, using the European Seasonal

[3] We thank T. Knutson and I. Held of National Oceanic and Atmospheric Administration/Geophysical Fluid Dynamics Laboratory (NOAA/GFDL) for suggesting this.

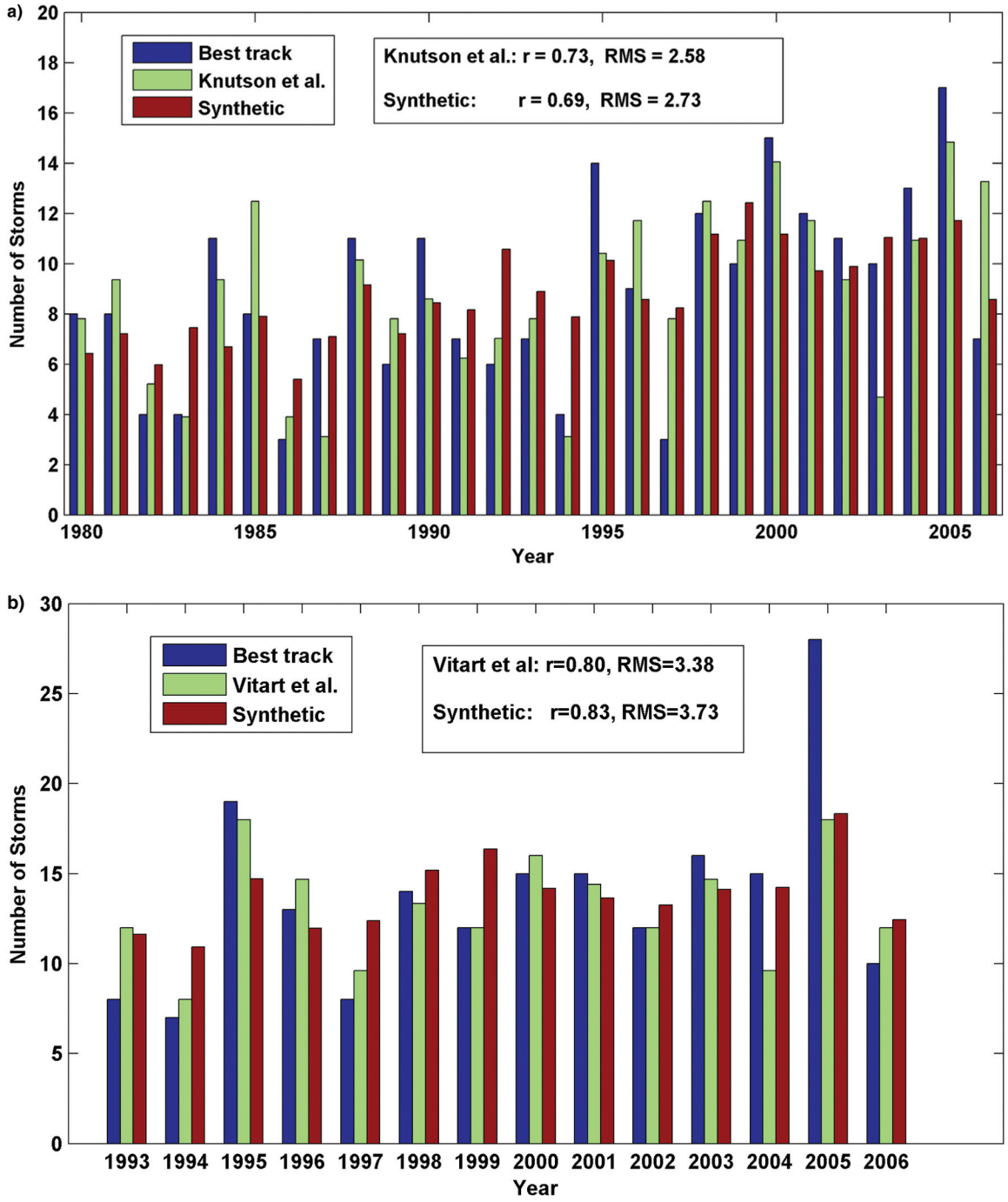

FIG. 4. Annual frequency of synthetic tropical cyclones in the North Atlantic (green bars) compared to best-track counts (blue bars) and to annual counts simulated by (a) Knutson et al. (2007) for the period of 1080–2006, and (b) Vitart et al. (2007) for the period of 1993–2006, shown in each case by red bars. The correlation coefficients (*r*) and root-mean-square errors (RMS) between the model and best-track storms are also indicated. The Knutson et al. simulations represent a single realization (their model 2), while the Vitart et al. count represents an ensemble median. Two hundred synthetic events were used each year. The data in (a) represent Aug–Oct storms only, while all events are included in (b). Note that subtropical events are included in the best-track data.

to Interannual Prediction (EUROSIP) multimodel ensemble of coupled ocean–atmosphere models. This consists of three models, and each model is initialized either 40 or 41 times to produce an ensemble. The models are initialized on the first day of each month and are used to forecast activity for

that month. Results were presented in which storms were reforecast for the period of 1993–2004, while real-time forecasts were used for 2005 and 2006. The ensemble median number of storms in each year is compared with our synthetic storm count in Fig. 4b. As with the comparison with the Knutson et al. (2007) results, our simulations are statistically very similar to those of Vitart et al. Because those results are based on one-month forecasts, any skill is attributable to the skill in forecasting the monthly mean states (including, possibly, the variances and covariances within those months) and not the details of day-to-day fluctuations, whose predictability time scale is somewhat less than a month. Our results, together with those of Vitart et al. and Knutson et al., suggest that as much as half of the interannual variability of Atlantic tropical cyclone activity can be attributed to the characteristics of the monthly mean state of the atmosphere and ocean, and not to the details of high-frequency fluctuations, such as African easterly waves. The residual root-mean-square error of between three and four storms per year is also consistent with the results of Sabbatelli and Mann (2007), who were able to attribute varying Atlantic storm counts to changing sea surface temperature and ENSO with a residual random component of between three and four storms per year.

Encouraged by these results, we simulated 200 events in each of the other four regions in each of the years from 1980 to 2006 and compared them to the observed events. Somewhat to our surprise, there is essentially no correlation between the simulated and observed annual frequencies of tropical cyclones anywhere outside the North Atlantic. This is perhaps related to the fact that while tropical cyclone frequency is well correlated with sea surface temperature in the North Atlantic (Mann et al. 2007), there is no indication of such a correlation elsewhere. We do find more significant correlations between best-track and simulated power dissipation, as shown in Fig. 5, which are consistent with the closer relationship between power dissipation and sea surface temperature, noted by Emanuel (2005a), even though power dissipation depends on both storm frequency and intensity, the latter of which is poorly estimated outside the North Atlantic region. The overall trend in simulated power dissipation agrees reasonably well with the trend deduced from best-track data in all basins except the eastern North Pacific, the only basin in which the best-track trend is downward. Over the 27-yr period, the simulated global power dissipation increases by 63%, versus an increase of 48% in the best-track data. Note, however, that outside the Atlantic, the simulated increases are not in agreement with the reanalysis of tropical cyclone power dissipation undertaken by Kossin et al. (2007), who found that power dissipation decreased everywhere except in the North Atlantic, and, marginally, in the western North Pacific.

The results presented in this section suggest that fairly realistic tropical cyclone climatologies can be derived from global data that realistically represent both the large-scale thermodynamic state of the tropical ocean and atmosphere and the large-scale kinematic state, including day-to-day variations in winds through the depth of the troposphere. The genesis-by-natural-selection technique described here also appears to give reasonable representations of the spatial, annual, interannual, and interdecadal variability of tropical cyclone activity, and is independent of historical tropical cyclone data, allowing one to estimate storm activity in different climate states, as described presently.

APPLICATION TO GLOBAL CLIMATE MODELS. Application of this technique to global climate models is straightforward, as long as it is possible to derive the same kinematic and thermodynamic quantities from these models as from the reanalysis data. This requires monthly mean sea surface and atmospheric temperature, and daily output of horizontal winds at 250 and 850 hPa, from which the variance and covariance matrices are extracted, as described in detail in the online supplement to Emanuel et al. (2006; online at ftp://texmex.mit.edu/pub/emanuel/PAPERS/hurr_risk_suppl.pdf). To examine the effect of global warming, in particular, we compare two sets of 2,000 events in each ocean basin driven by global climate simulations produced in aid of the most recent report of the IPCC (Solomon et al. 2007). The first set is based on simulations of the climate of the twentieth century, and the second on IPCC scenario A1b, for which atmospheric CO_2 concentration increases to 720 ppm by the year 2100 and then is held constant at that value. In each case, we accumulate daily output statistics for the last 20 yr of the simulation—1981–2000 for the twentieth-century simulations and 2181–2200 for the A1b simulations. Most of the data were obtained from the World Climate Research Program (WCRP) third Climate Model Intercomparison Project (CMIP3) multimodel dataset. This archive contains output from over 20 models run by 15 organizations, but at the time this study was conducted, we were only able to locate the required daily data from seven models, listed in Table 1.

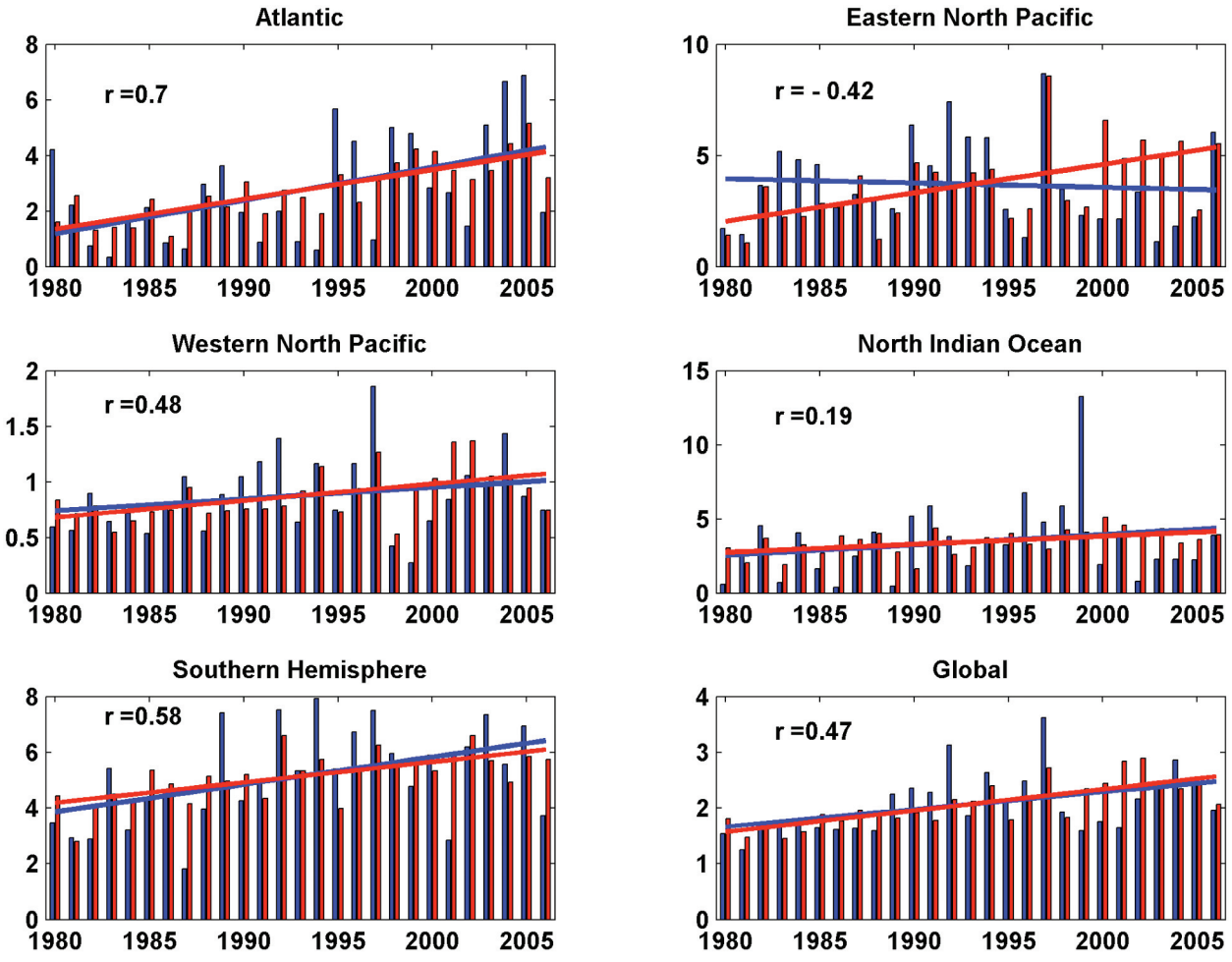

Fig. 5. Power dissipation index for each year from 1980 to 2006, from best-track data (blue) and simulations (red), for each basin and for the global total. The correlation coefficient between the best-track and simulated series is indicated in the upper-left corner of each panel, and the straight lines indicate the regression slopes of each series. Power dissipation units are 10^{11} m^3s^{-2} for the Atlantic, eastern North Pacific, and Southern Hemisphere, 10^{10} m^3s^{-2} for the north Indian Ocean, and 10^{12} m^3s^{-2} for the western North Pacific and global total.

The choice of the particular periods of time over which to accumulate climate model statistics to drive our downscaling method was motivated almost entirely by the availability of daily model output needed to derive the wind covariances. Given the noticeable multidecadal variability of some coupled climate models, even when driven with constant climate forcing (Delworth and Mann 2000), 20 yr is probably insufficient for averaging over such natural variations in the climate simulations, and so the comparison between the periods of 1981–2000 and 2181–2200 in any given model may be strongly affected if such variability is present. On the other hand, the particular time scales of multidecadal variability vary substantially from model to model (Delworth and Mann 2000), and so the ensemble of model results may nevertheless be representative of long-term climate change.

Calibration. The random seeding technique for genesis does not produce an absolute rate of genesis per unit time per unit area. To calibrate the technique, we set the global number of genesis events per year in each model to its observed global value in the period of 1981–2000 for each of the twentieth-century simulations. The calibration constants thus derived were then used for the A1b simulations. Thus, the annual, global twentieth-century genesis rates are set to observations, but the rates are free to vary spatially and seasonally, and to adjust to the different climate state of IPCC's A1b scenario.

Because different models have different convection schemes with different thermodynamic constants and assumptions, each produces slightly different temperature profiles in convecting regions, resulting in sometimes substantial differences in potential intensity, calculated using the algorithm

Table 1. Models used—origins, resolution, designation, and calibration.				
Model	**Institution**	**Atmospheric resolution**	**Designation in this paper**	**Potential intensity multiplicative factor**
Community Climate System Model, 3.0	National Center for Atmospheric Research	T85, 26 levels	CCSM3	1.2
CNRM-CM3	Centre National de Recherches Météorologiques, Météo-France	T63, 45 levels	CNRM	1.15
CSIRO-Mk3.0	Australian Commonwealth Scientific and Research Organization	T63, 18 levels	CSIRO	1.2
ECHAM5	Max Planck Institution	T63, 31 levels	ECHAM	0.92
GFDL-CM2.0	NOAA Geophysical Fluid Dynamics Laboratory	2.5°×2.5° 24 levels	GFDL	1.04
MIROC3.2	CCSR/NIES/FRCGC, Japan	T42, 20 levels	MIROC	1.07
mri_cgcm2.3.2a	Meteorological Research Institute Japan	T42, 30 levels	MRI	0.97

described in Bister and Emanuel (2002; the algorithm itself is available as a FORTRAN subroutine online at ftp://texmex.mit.edu/pub/emanual/TCMAX/). This can result in quite different cumulative frequency distributions of storm lifetime peak intensity among the various models when simulating the climate of the twentieth century. To correct for these model-to-model differences, we adjusted the potential intensities of each model by a single multiplicative constant in such a way as to minimize the differences in the cumulative frequency distributions of storm lifetime peak wind speeds. These multiplicative factors are listed in Table 1. Note that in this case, a single factor is applied to each model for all ocean basins. Because potential intensity affects the frequency of storms in our genesis technique, the calibration of potential intensity was done before the frequency calibration.

In summary, a frequency calibration factor was applied to each model's global annual genesis frequency, and each model's global potential intensity was likewise multiplied by a single factor. This guaranties that each model will produce roughly the correct cumulative frequency distribution of tropical cyclone lifetime peak wind speed in their simulations of the last 20 yr of the twentieth century. These calibrations are then held fixed in simulations of different climates.

Quality of twentieth-century simulations. The quality of the simulated storms can be assessed against historical tropical cyclone data using a variety of metrics. Here we choose to compare the spatial and seasonal variability on the synthetic storms driven from simulations of the last 20 yr of the twentieth-century climate to historical data. Departures of the simulated from the observed climatology may reflect imperfections of the technique itself, the model-simulated large-scale climates, or the climatological tropical cyclone data. For the latter, we used best-track data from the period of 1981–2006 inclusive; these data were obtained from the National Oceanic and Atmospheric Administration's National Hurricane Center for the Atlantic and eastern North Pacific (Jarvinen et al. 1984; Landsea et al. 2004), and from the U.S. Navy's Joint Typhoon Warning Center for the rest of the world. Note that we did not seed the South Atlantic in any of the simulations reported on here, owing to the very large amount of computational time required to produce a relatively low yield.

Figure 6 compares the spatial distribution of genesis points, integrated over the entire 20-yr period. For both the best-track and synthetic data, genesis is defined as the first point in the record where the peak 1-min wind at 10-m altitude equaled or exceeded 15 m s^{-1}. The upper-left panel pertains to best-track data, while the remaining seven panels show results from each of the global models. Although the grossest features of the observed distribution are well simulated by all the models, there are noticeable differences among the models. In general, the observed distribution is more concentrated in the eastern North Pacific, and except for the Centre National de Recherches Météorologiques (CNRM) and Model for Interdisciplinary Research on Climate (MIROC) models, there is too much activity in the central North Pacific. Aside from these fairly systematic errors, each model has its own strengths and weaknesses in simulating the late-twentieth-century genesis distribution. For example, the third Community

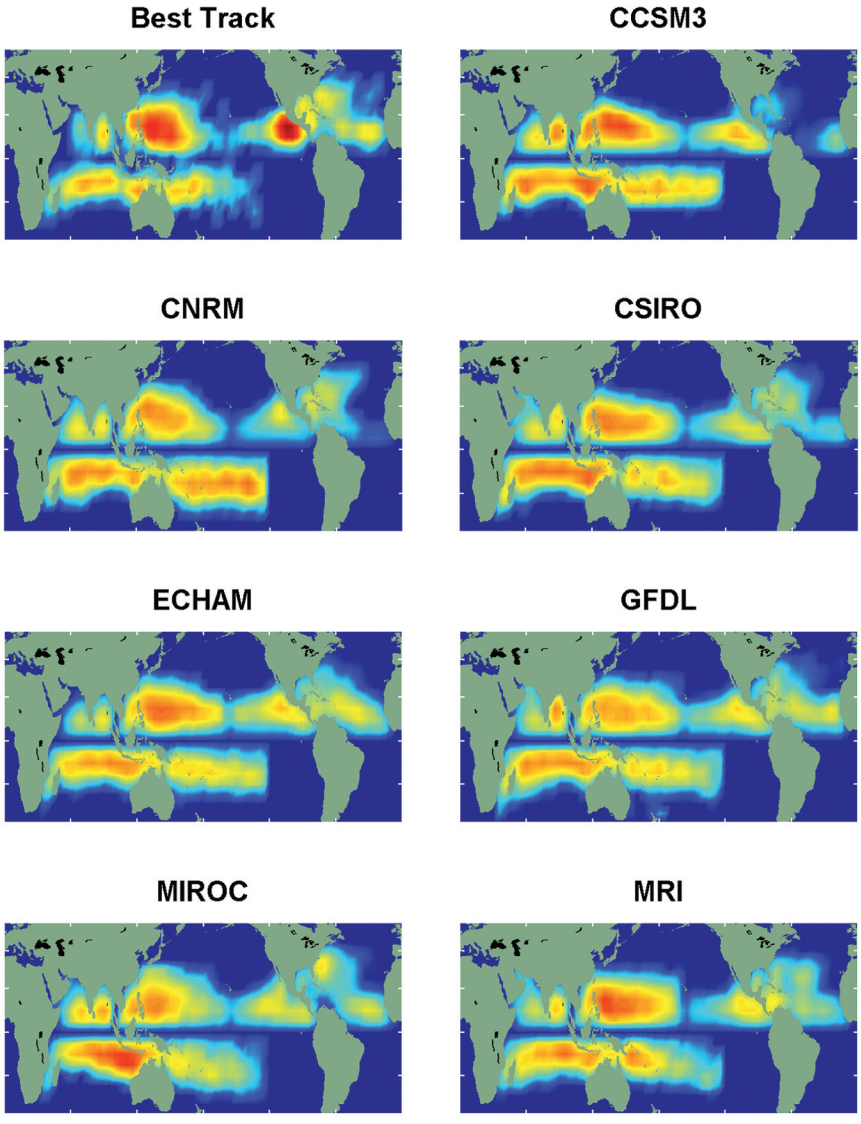

Fig. 6. Annual genesis distributions during the period of 1981–2006 for best-track data (upper-left) and for each of the seven models considered in this study. Shown is the logarithm of 1 + the genesis density accumulated over a 5° × 5° grid; the color scale is the same in each case and identical to that used in Figs. 1a,b. The model genesis distributions are based on 2,000 synthetic storms in each of the Atlantic, eastern North Pacific, western North Pacific, northern Indian, and Southern Hemisphere regions, while the best-track data for this period include 303, 439, 773, 129, and 716 events in the respective regions.

Climate System Model (CCSM3) has practically no activity in the North Atlantic.

Figure 7 compares the annual cycle of genesis in each of the seven models to historical data in each of the five basins considered here. Again, the gross features of the seasonal variability are captured by most of the models, but there are interesting systematic errors. In the eastern North Pacific, there are too few synthetic storms in June and July, and far too many in October–December. In general, except in the Atlantic, the models produce too many storms in winter and not enough in summer. Likewise, in the northern Indian Ocean, the models produce too many storms during the midsummer lull in activity, when there are very few storms in nature. Here, however, the observed distribution is calculated from only a small number of events in the 1981–2000 period, so care must be exercised in assessing the statistical significance of the comparison.

A general impression from these results is that the models underestimate the sensitivity of tropical genesis rates in climate variability, at least as measured by seasonal and spatial variability. The distributions in both space and time are not as sharply peaked as the distributions calculated from historical tropical cyclone data. Again, this may be because the models may underpredict the spatial and seasonal variability of the resolved climate, or because of defects in the genesis-by-natural-selection technique. Nevertheless, the gross features of the observed spatial and seasonal variability of genesis rates are sufficiently well simulated to make an examination of the sensitivity of simulated tropical cyclone activity to global climate worthwhile.

To assess the possibility that 20 yr is insufficient for averaging out natural multidecadal variability in the models, we obtained data from the period 1961–80 for the GFDL model to compare to the simulations driven using data from 1981 to 2000. Simulated tropical cyclone activity was substantially less in the earlier period, with frequency as little

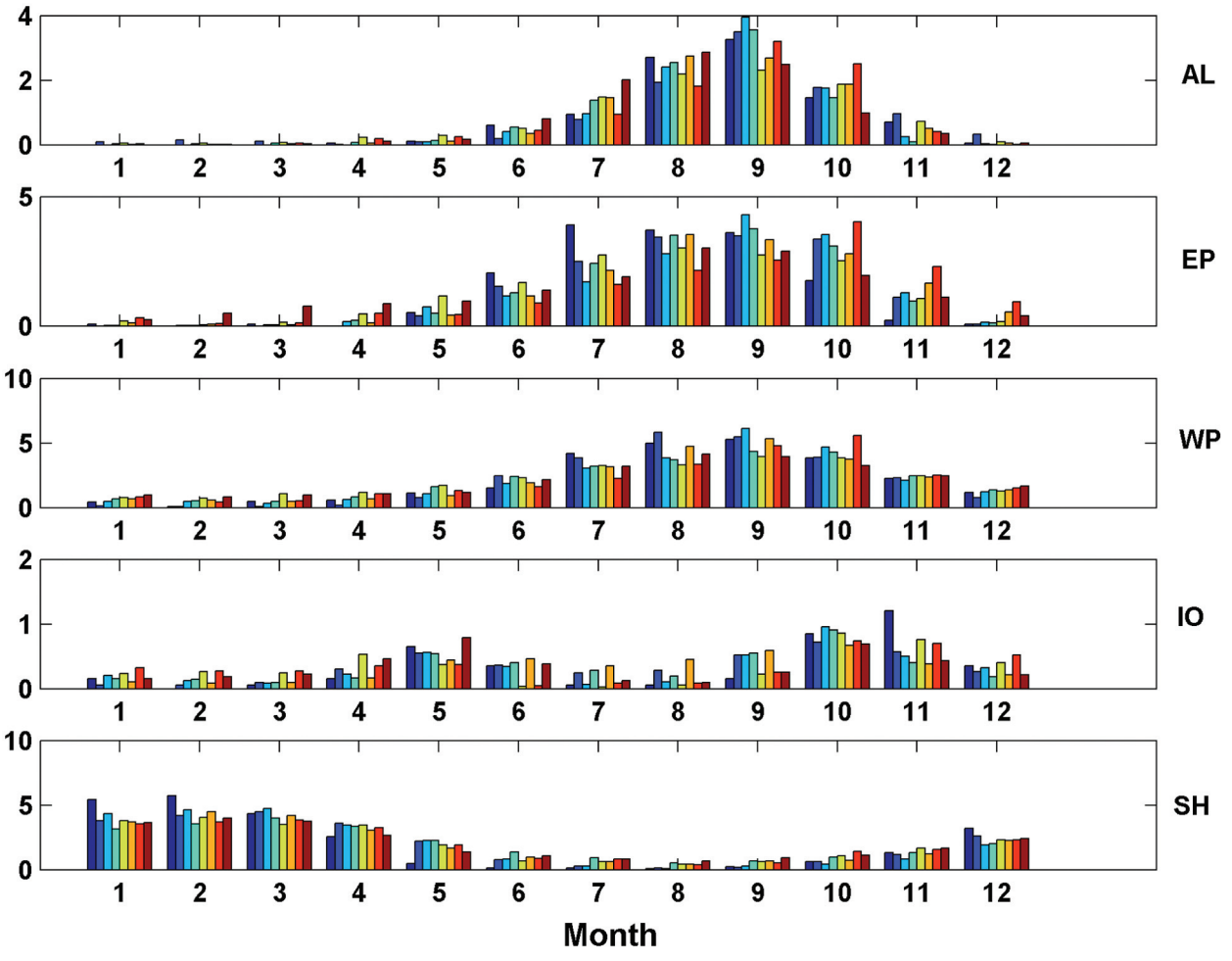

Fig. 7. Annual cycle of tropical cyclone counts during the period of 1981–2000, for each of the five main tropical cyclone regions (from top to bottom). The colored bars represent (from left to right) best-track data and synthetic storms driven by output from the CCSM3, CNRM, CSIRO, ECHAM, GFDL, MIROC, and MRI models. The annual total for each model is constrained to equal the observed annual total in each basin; the observed basin counts are given in the caption to Fig. 6.

as half as great in some regions. This suggests that comparisons between 20-yr periods in the twentieth and twenty-second centuries for at least some models may be seriously affected by multidecadal variability, a point we shall return to presently. Note that while the full range of radiative forcing variability owing to greenhouse gases, aerosols, and volcanoes was included in the simulation, the natural, multidecadal variability of the model would not necessarily have had the correct phase relationship with any such variability in nature.

Comparison of late-twentieth-century to late-twenty-second-century-tropical cyclone activity. Climate change affects simulated tropical cyclone activity by changing the space–time probability of genesis, the tracks taken by the simulated storms, and their intensity evolution. These, in turn, affect the peak intensity achieved by the storms, their duration, and their spatial distributions. In the following, we compare certain key statistics of simulated activity in the last 20 yr of the twenty-second century, compared to the last 20 yr of the twentieth century.

Figure 8a shows the change in overall tropical cyclone power dissipation index by model and basin. The power dissipation index was defined by Emanuel (2005a) as the integral over the lifetime of each storm of the maximum surface winds speed cubed; this is a measure of the total amount of kinetic energy dissipated by surface friction over the lifetime of the storm. Here we accumulate the power dissipation over each basin and over the 20-yr period in question. The change is expressed as 100 times the logarithm of the ratio of the power dissipation values in the two simulations; for small differences, this is approximately the percentage change. In general,

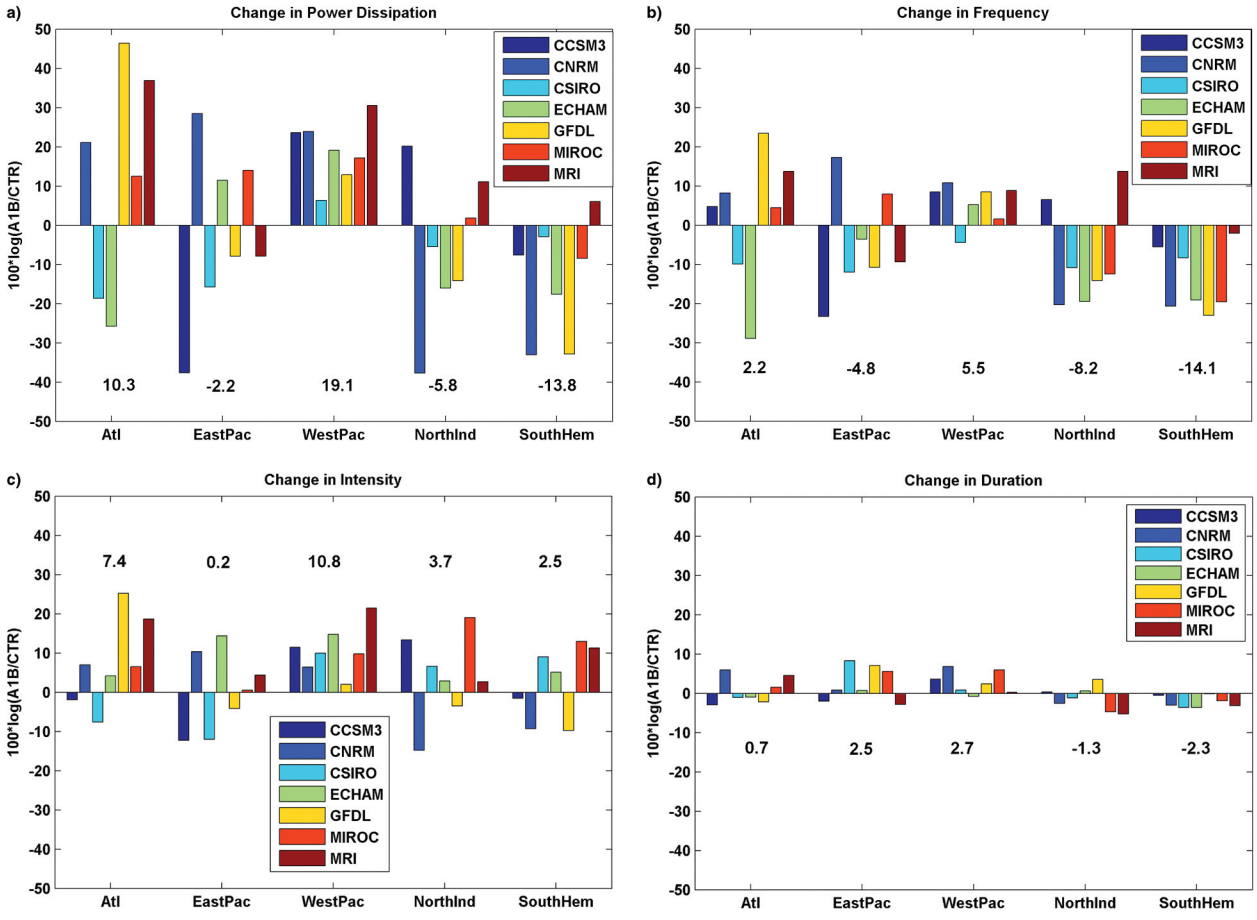

Fig. 8. Change in basinwide tropical cyclone (a) power dissipation, (b) frequency, (c) intensity, and (d) duration from the last 20 yr of the twentieth century to the last 20 yr of the twenty-second century, as predicted by running 2,000 synthetic events in each basin in each period of 20 yr. The different colors correspond to the different global climate models, as given in the legends. See text for definitions of intensity and duration. The change here is given as 100 multiplied by the logarithm of the ratio of twenty-second- and twentieth-century quantities. Note that (a) is the sum of (b)–(d). The values of the changes averaged across all models are given by the numbers in black.

there are substantial increases in power dissipation in the western North Pacific and decreases in the Indian Ocean and through the Southern Hemisphere, while the tendency is somewhat indeterminate in the eastern North Pacific, with large variability from one model to the next. Four out of the seven models show appreciable increases in the North Atlantic, with the remaining three showing no change or decreases.

Figure 8b shows the percentage change in the frequency of all events that achieve a peak wind speed of at least 21 m s^{-1}. There is a general tendency toward decreasing frequency of events in the Southern Hemisphere, but the percentage change in frequency is not usually as large as the decrease in power dissipation, showing that the latter is also affected by decreasing intensity and/or duration. Changes in overall frequency in the eastern North Pacific are indeterminate, but six out of seven models show increases in the western North Pacific and five out of seven models show increasing frequency in the North Atlantic. Overall, the tendency of storm frequency is somewhat indeterminate in the Northern Hemisphere, but declines in the Southern Hemisphere.

Changes in the mean duration and intensity of events are shown in Figs. 8c,d. Here we follow Emanual (2007) in defining duration as

$$D \equiv \frac{1}{N}\sum_{i=1}^{N}\frac{\int_0^{\tau_i} V^i_{\max}\,dt}{V^i_{s\max}}, \qquad (1)$$

where N is the sample size, $V^i_{\max}$ is the maximum wind of storm i at any given time, $V^i_{s\max}$ is the lifetime maximum wind of storm i, and τ_i is the lifetime of each storm. This velocity-weighted duration assigns relatively little weight to long periods at which storms

sometimes exist at low intensity. The mean intensity is defined as

$$I \equiv \frac{\sum_{i=1}^{N} \int_0^{\tau_i} V_{\max}^3 \, dt}{ND}. \quad (2)$$

This is the mean cube of the maximum wind speed accumulated over the lifetime of each storm, divided by the duration as defined by (1). Note that the power dissipation is just the product of the overall frequency, duration, and intensity as defined above; thus, the logarithms of these quantities are additive and Figs. 8b–d add up to Fig. 8a, Fig. 8d shows little change in the velocity-weighted duration of events, but with a tendency toward decreasing duration in the Southern Hemisphere and north Indian Ocean, and slight increases elsewhere. As expected from theory and previous numerical simulations, there is an overall tendency toward increased intensity of storms, but some models show decreases in some basins.

We also calculated basin-averaged changes in sea surface temperature and potential intensity, defining the averaging areas to coincide roughly with conventional definitions of tropical cyclone main development regions. Curiously, there is no systematic correlation between changes in any of the metrics described in this section with changes in either sea surface temperature or potential intensity averaged over the individual basins. This contrasts sharply with the high correlation between variations in observed Atlantic tropical cyclone power dissipation and sea surface temperature, reported by Emanuel (2005a), and the relatively high correlation among year-to-year variability of power dissipation, sea surface temperature, and potential intensity in the simulations forced by reanalysis data in the years of 1980–2006. Deconvolving the various environmental factors responsible for the changes in the various tropical cyclone metrics described here is the subject of ongoing work and will be reported in the near future.

Changes in the spatial patterns of genesis are shown in Fig. 9 for each of the seven models and the average over all models. While there is much variation from one model to the next, several patterns emerge in the consensus that seem common to most models. As noted before, most models show declining frequency throughout the Southern Hemisphere, except for small regions east of Indonesia and the far western south Indian Ocean. Many individual models, as well as the model consensus, show increased frequency in the northern and western Arabian Sea, but decreased frequency in the Bay of Bengal and in the eastern and far western portion of the North Pacific, while there is some indication of increasing activity in the main development region of the western North Pacific. The model consensus has slightly decreased frequency of events in the Caribbean and in the western portion of the Atlantic main development region, with a noticeably increased frequency in the far eastern portion of the tropical Atlantic and in the subtropics, including off the southeast U.S. coast.

These results suggest potentially substantial changes in destructiveness of tropical cyclones as a consequence of global warming. But large model-to-model variability and natural multidecadal variability within at least some of the models also suggests large uncertainty in such projections, reflecting the uncertainties of climate model projections in general and the influence of natural variability. Ideally, we would like to compare simulations driven by climate model data accumulated over periods long enough both to quantify and account for the effects of natural variability, but because such data are not currently available, this is left to future work.

DISCUSSION. The findings presented here are largely consistent with those obtained by direct simulation of tropical cyclones by global models as well as by downscaling using regional models embedded in global models. The majority of such exercises to date show a decrease in global genesis rates, as summarized, for example, by Bengtsson et al. (2007). For example, recent global model-based studies (e.g., Bengsson et al. 1996; Sugi et al. 2002; Oouchi et al. 2006; Yoshimura et al. 2006; Bengtsson et al. 2007) all show decreasing frequency of tropical cyclones globally, although some studies show regional increases. This is encouraging, because the route to genesis in the method described here is quite different from that operating in climate models; one potentially serious limitation of our technique is the assumed constant amplitude and frequency of potential initiating disturbances. Because tropical cyclones evidently arise from finite-amplitude instability (Emanuel 1989), the prevalence and characteristics of potential initiating disturbances should be important, and these can be expected to depend on the climate state. At the same time, this limitation might be expected also to affect the quality of the seasonal cycle of tropical cyclone activity, yet the technique does reasonably well with this (see Fig. 3).

Some of the biases evident in the distributions of genesis events (see Fig. 6) are also common to explicitly produced events in climate models. For

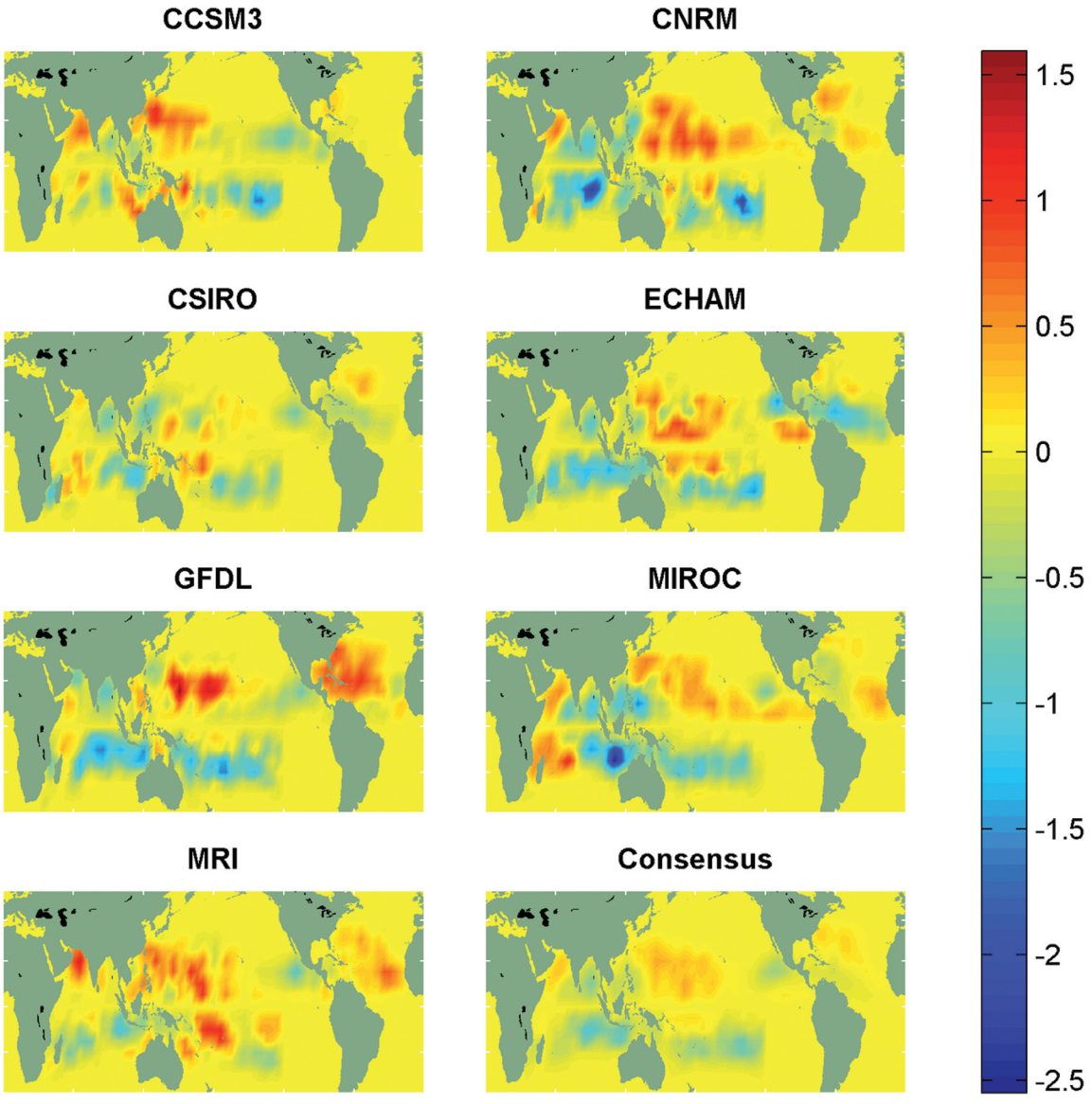

Fig. 9. Change in genesis density from the last 20 yr of the twentieth century to the last 20 yr of the twenty-second century, as predicted by running 2,000 synthetic events in each basin in each period of 20 yr for the (a) North Atlantic and (b) each model and for the average ("consensus") over all models. Each panel represents the results from a particular global model. The color scale is the same for all figures and is in units of number of events per 5° lat–lon square yr^{-1}.

example, it is common to produce too many events in the central North Pacific, and the geographic distributions are generally broader than observed (Camargo et al. 2005). This suggests that some of the defects in the genesis distributions noted here can be attributed to biases in the large-scale environment, though others no doubt arise from the assumption of uniform or vorticity-weighted seeding amplitude.

Of particular interest is the recent work by Bengtsson et al. (2007), who used one of the models (ECHAM5) included in this study; thus a direct comparison can be made. The time periods examined differ, however; whereas the present study compares the last 20 yr of the twentieth and twenty-second centuries, the Bengtsson et al. study compares the last 30 yr of the twentieth and twenty-first centuries. Because in scenario A1b, CO_2 does not level off until the year 2100, some additional warming will have occurred by the end of the twenty-second century. The output used to drive the synthetic tracks shown here was taken from the T63 version of ECHAM5; Bengtsson et al. also report T63 results, but examined

higher-resolution output as well. Curiously, the genesis distributions produced directly by ECHAM5 also show too many events in the central North Pacific (see their Fig. 6a), as does the present technique (Fig. 6 herein). Both techniques predict decreases in the frequency of events in all basins, except that our technique predicts a modest increase in the western North Pacific. As in the present study (Fig. 8c), the intensity distributions shown by Bengtsson et al. exhibit a tendency for increased frequency of the higher-intensity events, and this becomes more pronounced at higher spatial resolution. Note, however, that in these and the other direct GCM simulations, the intensity distributions of explicitly modeled storms are truncated at the high end compared to nature, probably because of the relatively low horizontal resolution of the model.

Thus, the present results are broadly consistent with those of global model studies in that both generally show an increased frequency of very intense storms, but some tendency toward a reduction in the overall frequency of events in the Southern Hemisphere. The simplicity of the intensity model and natural selection technique employed here allows us to draw a fairly definitive conclusion about why the frequency of events declines in some places in our simulations.

An important nondimensional parameter in the CHIPS intensity model is the normalized difference between the moist entropy of the middle troposphere and that of the boundary layer. This parameter, called χ_m in the various papers that describe the model (Emanuel 1989, 1995), was shown to be important in regulating how long it takes an initial disturbance to moisten the middle troposphere to the point that intensification can occur; the larger it is, the longer the gestation period.

The specific definition of χ_m is

$$\chi_m \equiv \frac{s_b - s_m}{s_0^* - s_b}, \tag{3}$$

where s_m, s_b, and s_0^* are the entropies of the middle troposphere and boundary layer, and the saturation entropy of the sea surface, respectively. The moist entropy is defined (Emanuel 1994) as

$$s \equiv c_p \ln T - R_d \ln p + \frac{L_v q}{T} - R_v q \ln \mathrm{H}, \tag{4}$$

where for simplicity we have neglected the dependence of the heat capacities and gas constants on the water content. Here c_p is the heat capacity at constant pressure of air, L_v is the latent heat of vaporization, q is the specific humidity, R_d is the gas constant for dry air, R_v is the gas constant for water vapor, and H is the relative humidity.

The quantity χ_m measures the relative importance of downdrafts and surface fluxes in controlling the entropy of the subcloud layer. It is an important parameter in the formulation of the boundary layer quasi-equilibrium closure for convective updraft mass fluxes used in the CHIPS model and elsewhere (Emanuel 1995). For example, in CHIPS, the convective updraft mass flux is given by

$$M_u = w + {C_k |\mathbf{V}|}\Big/{\chi_m}, \tag{5}$$

where w is the large-scale vertical velocity at the top of the boundary layer, C_k is the surface exchange coefficient for enthalpy, and $|\mathbf{V}|$ is the surface wind speed. Thus, χ_m also determines the rates of increase of convective updraft with surface wind.

The CHIPS model has only one layer in the middle troposphere, in which χ_m is defined. When it is run in forecast mode, or used in the synthetic track technique, s_m is defined at 600 hPa, which is usually close to the level at which it attains a minimum value in the tropics.

In regions susceptible to tropical cyclones, the atmosphere is approximately neutral to moist convection and the lapse rate of the troposphere is nearly moist adiabatic. Thus,

$$s_b \cong s^*, \tag{6}$$

where s^* is the (approximately constant with height) saturation entropy of the troposphere above the boundary layer. Thus, it should not matter at which level we choose to calculate it, so we again choose 600 hPa. Using the definition of moist entropy (see, e.g., Emanuel 1994), the numerator in (3) can then be approximated as

$$s_b - s_m \cong s^* - s_m = \frac{L_v q^*}{T}(1 - \mathrm{H}) + R_v \mathrm{H} q^* \ln \mathrm{H}, \tag{7}$$

where q^* is the saturation specific humidity and the quantities are evaluated at 600 hPa.

The quantity q^* does not vary much in the tropics, either in space or with time, because of the strong dynamical constraint on the magnitude of the temperature gradient, owing to the small value of the Coriolis parameter. Thus, in the present climate, seasonal and spatial variations in $s_b - s_m$ as given by (7) are dominated by variations in relative humidity. But, under global warming, changes in χ_m at fixed points in space are dominated by changes in q^*, while the relative humidity stays approximately constant (at least in

most climate models). In fact, globally, we can predict that the magnitude of χ_m should generally increase with global warming, because its numerator scales with q^* (Clausius–Clapeyorn), while its denominator is essentially proportional to surface evaporation (at fixed surface wind speed) and so should only increase slowly with warming, because it is bounded above by insolation, which does not change much.

The magnitude of χ_m does indeed increase almost everywhere in most global climate simulations of global warming, and this reduces the rates of tropical cyclogenesis under global warming using the seeding and natural selection method described here. Figure 10 shows the percentage increase in frequency of events globally in an experiment in which q^* was held fixed in (7).[4] In this case, χ_m generally decreases, owing to the increase in $s_0^* - s_b$, and thus the frequency of tropical cyclone genesis generally increases. This suggests an important role for χ_m in regulating tropical cyclone frequency. The increase of its magnitude under global warming may very well also provide an explanation for the decrease in explicit genesis rates in most climate models. Because, according to (5), the moist convective updraft mass flux should vary inversely with χ_m as given by (3), rates of tropical cyclogenesis should also covary, to some extent, with moist convection in general. Note, however, that the dry static stability along a moist adiabat increases with temperature, so that in the warming by convection, which is broadly the product of the convective mass flux and the dry stability, there is a partial compensation for decreased mass flux in the increased stability.

[4] The comparison here is for two sets of simulations that were performed earlier in the course of the research that led to this paper. They differ from the ones described here in using an unmodified parameterization of shear in the CHIPS model. The differences are small, and so we expect that the results presented here would differ very little had we used the modified shear parameterization.

SUMMARY. A new technique for downscaling tropical cyclone climatologies from global analyses and models has been described. The technique begins with the random seeding of all ocean basins with weak, warm-core vortices whose motion is determined by a beta-and-advection model and whose intensity is found using a coupled ocean–atmosphere numerical model. The winds used to drive the track model and the winds, sea surface temperatures, and atmospheric temperature needed by the intensity model are all derived from the global model or reanalysis fields. The great majority of the initial seeds perish without achieving tropical storm strength, owing to low potential intensity, low midtropospheric humidity, and/or too much wind shear. The climatology of the surviving storms shows reasonable agreement with the spatial, seasonal, and interannual variability of observed storms, and some improvement is attained by weighting the seeding density with the large-scale, monthly mean, low-level vorticity. The absolute, global annual frequency of the synthetic storms is calibrated for each model/reanalysis by the observed global annual frequency, while the potential intensity is calibrated by a single multiplicative factor for each model/reanalysis so as to obtain a reasonable distribution of storm intensities.

Simulated storms driven by reanalysis data in the period 1980–2006 show reasonable agreement with observed storms, including their spatial variability and temporal variability on time scales from seasons to decades. In the Atlantic, interannual variability of storm frequency responds reasonably well to ENSO

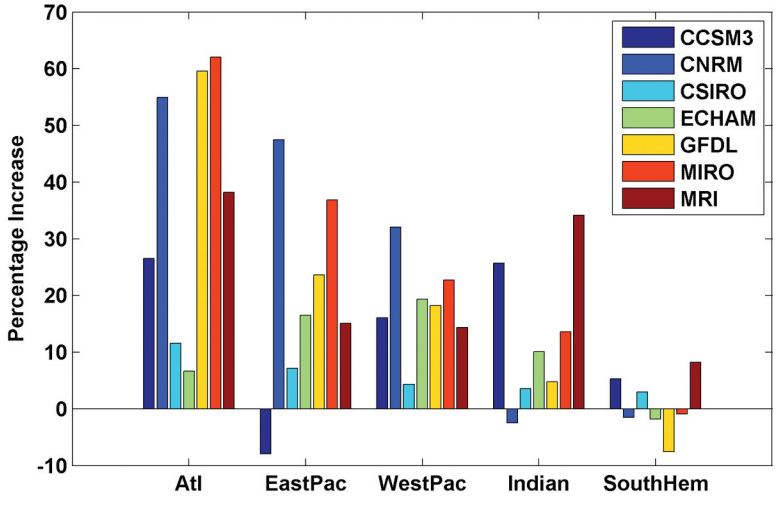

Fig. 10. Percentage increase in basin-wide tropical cyclone frequency from the last 20 yr of the twentieth century to the last 20 yr of the twenty-second century, as predicted by running 2,000 synthetic events in each basin in each period of 20 yr. The different colors correspond to the different global climate models, as given in the legends. In this experiment, the saturation mixing ratio q^* was held to a fixed constant value in (4); this should be contrasted with Fig. 8b in which q^* was permitted to vary with climate change.

and is highly correlated with observed interannual variability, but such correlation is not obtained outside the Atlantic. Simulated power dissipation increases over the period in all basins, and is in reasonable agreement with observed power dissipation except in the eastern North Pacific.

The technique is then applied to the output of seven global climate models run in support of the most recent IPCC report, chosen mostly on the basis of the availability of daily output needed to drive the wind covariances matrices used by the technique. Two thousand tropical cyclones in each of 5 basins were simulated using global model data from the last 20 yr of the twentieth century, and the last 20 yr of the twenty-second century as simulated by assuming IPCC emission scenario A1b. These simulations show potentially large changes in tropical cyclone activity in response to global warming, though the sign and magnitude of the changes vary a great deal from basin to basin and from model to model, reflecting large regional differences in the global model predictions as well as natural multidecadal variability in each model that cannot be averaged out over the 20-yr periods considered here. There is an overall tendency toward decreasing frequency of events in the Southern Hemisphere, consistent with direct simulations of tropical cyclones using global climate models, and power dissipation and storm intensity generally increase, as expected from theory and prior work with regional tropical cyclone models. On the other hand, there is a tendency toward increased frequency of events in the western North Pacific.

It is noteworthy that simulated global tropical cyclone power dissipation increases by more than 60% in simulations driven by NCAR–NCEP reanalysis over the period of 1980–2006, consistent with deductions from best-track data, while global power dissipation increases somewhat more than that over the next 200 yr in simulations driven by climate models undergoing global warming. This suggests either that the greater part of the large global increase in power dissipation over the past 27 yr cannot be ascribed to global warming, or that there is some systematic deficiency in our technique or in global models that leads to the underprediction of the response of tropical cyclones to global warming. As shown by comparing Figs. 8b to 10, the predicted global changes in storm frequency depends on a rather simplistic representation of the vertical distribution of moist entropy in the atmosphere as represented by the parameter χ_m, defined by (3). Because χ_m varies little within the tropics in the present climate, it is difficult to test the sensitivity to it against real data. Yet the predicted change in storm frequency is broadly consistent with explicit predictions using global climate models, at least in the Southern Hemisphere.

We are in the process of further analyzing the physical reasons for the predicted changes in activity described here, and will report on the results of this effort in the near future.

ACKNOWLEDGMENTS. The authors thank Isaac Held, Tom Knutson, Chris Landsea, and an anonymous reviewer for helpful comments on this work. Frederic Vitart graciously provided the median Atlantic storm counts for the comparison presented in Fig. 4b. We also thank the modeling groups for making their simulations available for analysis, the Program for Climate Model Diagnosis and Intercomparison (PCMDI) for collecting and archiving the CMIP3 model output, and the WCRP's Working Group on Coupled Modeling (WGCM) for organizing the model data analysis activity. The WCRP CMIP3 multimodel dataset is supported by the Office of Science, U.S. Department of Energy. The first author was supported by Grant ATM-0432090 from the National Science Foundation. The third author was supported by a graduate fellowship from the American Meteorological Society and the National Weather Service.

REFERENCES

Bengtsson, L., M. Botzet, and M. Esch, 1996: Will greenhouse-induced warming over the next 50 years lead to higher frequency and greater intensity of hurricanes? *Tellus,* **48A,** 57–73.

——, K. I. Hodges, M. Esch, N. Keenlyside, L. Kornbleuh, J.-J. Luo, and T. Yamagata, 2007: How may tropical cyclones change in a warmer climate? *Tellus,* **59A,** 539–561.

Bister, M., and K. A. Emanuel, 1998: Dissipative heating and hurricane intensity. *Meteor. Atmos. Phys.,* **50,** 233–240.

——, and ——, 2002: Low frequency variability of tropical cyclone potential intensity 1. Interannual to interdecadel variability. *J. Geophys. Res.,* **107,** 4801, doi:10.1029/2001JD000776.

Bove, M. C., J. O'Brien, J. B. Elsner, C. W. Landsea, and X. Niu, 1998: Effect of El Niño on U.S. landfalling hurricanes, revisited. *Bull. Amer. Meteor. Soc.,* **79,** 2477–2482.

Camargo, S. J., A. G. Barnston, and S. E. Zebiak, 2005: A statistical assessment of tropical cyclone activity in atmospheric general circulation models. *Tellus,* **57A,** 589–604.

——, K. A. Emanuel, and A. H. Sobel, 2007: Use of a genesis potential index to diagnose ENSO effects on tropical cyclone genesis. *J. Climate,* **20,** 4819–4834.

Chan, J. C. L., 1985: Tropical cyclone activity in the northwest Pacific in relation to the El Niño/Southern Oscillation phenomenon. *Mon. Wea. Rev.,* **113,** 599–606.

——, 2006: Comments on "Changes in tropical cyclone number, duration, and intensity in a warming environment." *Science,* **311,** p. 1713.

——, and J.-E. Shi, 1996: Long-term trends and interannual variability in tropical cyclone activity over the western North Pacific. *Geophys. Res. Lett.,* **23,** 2765–2767.

Chang, E. K. M., and Y. Guo, 2007: Is the number of North Atlantic tropical cyclones significantly underestimated prior to the availability of satellite observations? *Geophys. Res. Lett.,* **34,** L14801, doi:10.1029/2007GL030169.

Chen, S. S., J. F. Price, W. Zhao, M. A. Donelan, and E. J. Walsh, 2007: The CBLAST-Hurricane program and the next-generation fully coupled atmosphere–wave–ocean models for hurricane research and prediction. *Bull. Amer. Meteor. Soc.,* **88,** 311–317.

Curry, J. A., P. J. Webster, and G. J. Holland, 2006: Mixing politics and science in testing the hypothesis that greenhouse warming is causing a global increase in hurricane intensity. *Bull. Amer. Meteor. Soc.,* **87,** 1025–1037.

Delworth, T. L., and M. E. Mann, 2000: Observed and simulated multidecadal variability in the Northern Hemisphere. *Climate Dyn.,* **16,** 661–676.

Donnelly, J. P., and J. D. Woodruff, 2007: Intense hurricane activity over the past 5000 years controlled by El Niño and the West African monsoon. *Nature,* **447,** 465–468.

Elsner, J. B., B. H. Bossak, and X.-F. Niu, 2001: Secular changes to the ENSO-U.S. hurricanes relationship. *Geophys. Res. Lett.,* **28,** 4123–4126.

Emanuel, K. A., 1986: An air-sea interaction theory for tropical cyclones. Part I: Steady-state maintenance. *J. Atmos. Sci.,* 4**3,** 585–605.

——, 1987: The dependence of hurricane intensity on climate. *Nature,* **326,** 483–485.

——, 1989: The finite-amplitude nature of tropical cyclogenesis. *J. Atmos. Sci.,* **46,** 3431–3456.

——, 1994: *Atmospheric Convection.* Oxford University Press, 580 pp.

——, 1995: The behavior of a simple hurricane model using a convective scheme based on subcloud-layer entropy equilibrium. *J. Atmos. Sci.,* **52,** 3959–3968.

——, 2005a: Increasing destructiveness of tropical cyclones over the past 30 years. *Nature,* **436,** 686–688.

——, 2005b: Meteorology: Emanuel replies. *Nature,* **438,** E13.

——, 2006: Climate and tropical cyclone activity: A new model downscaling approach. *J. Climate,* **19,** 4797–4802.

——, S. Ravela, E. Vivant and C. Risi, 2006: A statistical-deterministic approach to hurricane risk assessment. *Bull. Amer. Meteor. Soc.,* **19,** 299–314.

——, 2007: Environmental factors affecting tropical cyclone power dissipation. *J. Climate,* **20,** 5497–5509.

——, and D. S. Nolan, 2004: Tropical cyclone activity and the global climate system. Preprints, *26th Conf. on Hurricanes and Tropical Meteorology,* Miami, FL, Amer. Meteor. Soc., 10A.2.

——, C. DesAutels, C. Holloway, and R. Korty, 2004: Environmental control of tropical cyclone intensity. *J. Atmos. Sci.,* **61,** 843–858.

Frappier, A. B., T. R. Knutson, K.-B. Liu, and K. Emanuel 2007: Perspective: Coordinating paleoclimate research on tropical cyclones with hurricane–climate theory nd modelling. *Tellus,* **59A,** 529–537.

Goldenberg, S. B., C. W. Landsea, A. M. Mestas-Nuñez, and W. M. Gray, 2001: The recent increase in Atlantic hurricane activity: Causes and implications. *Science,* **293,** 474–479.

Gray, W. M., 1979: Hurricanes: Their formation, structure, and likely role in the tropical circulation. *Meteorology over the Tropical Oceans,* D. B. Shaw, Ed., Royal Meteorological Society, 155–218.

——, 1984: Atlantic seasonal hurricane frequency. Part I: El Niño and 30 mb quasi-biennial oscillation influences. *Mon. Wea. Rev.,* **112,** 1649–1668.

Hoyos, C. D., P. A. Agudelo, P. J. Webster, and J. A. Curry, 2006: Deconvolution of the factors contributing to the increase in global hurricane intensity. *Science,* **312,** 94–97.

Jarvinen, B. R., J. Neumann, and M. A. S. Davis, 1984: A tropical cyclone data tape for the North Atlantic Basin, 1886–1983: Contents, limitations, and uses. NOAA Tech. Memo. NWS NHC 22, 21 pp.

Knutson, T. R., and R. E. Tuleya, 2004: Impact of CO_2-induced warming on simulated hurricane intensity and precipitation: Sensitivity to the choice of climate model and convective parameterization. *J. Climate,* **17,** 3477–3495.

——, ——, and Y. Kurihara, 1998: Simulated increase of hurricane intensities in a CO_2-warmed climate. *Science,* **279,** 1018–1020.

——, J. J. Sirutis, S. T. Garner, I. M. Held and R. E. Tuleya, 2007: Simulation of the recent multi-decadal increase of Atlantic hurricane activity using an 18-km-grid regional model. *Bull. Amer. Meteor. Soc.,* **88,** 1549–1565.

Kossin, J. P., K. R. Knapp, D. J. Vimont, R. J. Murnane, and B. A. Harper, 2007: A globally consistent reanalysis of hurricane variability and trends. *Geophys. Res. Lett.,* **34,** L0481, doi:10.1029/2006GL028836.

Landsea, C. W., 2005: Hurricanes and global warming. *Nature,* **438,** E11–E12.

——, 2007: Counting Atlantic tropical cyclones back to 1900. *Eos, Trans. Amer. Geophys. Union,* **88,** 197–200.

——, and Coauthors, 2004: The Atlantic hurricane database re-analysis project: Documentation for the 1851–1910 alterations and additions to the HURDAT database. *Hurricanes and Typhoons: Past, Present and Future,* R. J. Murnane and K.-B. Liu, Eds., Columbia University Press, 177–221.

——, B. A. Harper, K. Hoarau, and J. A. Knaff, 2006: Can we detect trends in extreme tropical cyclones? *Science,* **313,** 452–454.

Liu, K.-B., and M. L. Fearn, 1993: Lake-sediment record of late Holocene hurricane activities from coastal Alabama. *Geology,* **21,** 793–796.

Malmquist, D. L., 1997: Oxygen isotopes in cave stalagmites as a proxy record of past tropical cyclone activity. *Proc. 22nd Conf. on Hurricanes and Tropical Meteorology,* Fort Collins, CO, Amer. Meteor. Soc., 393–394.

Mann, M. E., K. A. Emanuel, G. L. Holland, and P. J. Webster, 2007: Atlantic tropical cyclones revisited. *Eos, Trans. Amer. Geophys. Union,* 349–350.

Miller, D. L., C. I. Mora, H. D. Grissino-Mayer, C. J. Mock, M. E. Uhle, and Z. Sharp, 2006: Tree-ring isotope records of tropical cyclone activity. *Proc. Natl. Acad. Sci.,* **103,** 14 294–14 297.

Nott, J. F., 2003: Intensity of prehistoric tropical cyclones. *J. Geophys. Res.,* **108,** 4212, doi:10.1029/2002JD002726.

Oouchi, K., J. Yosimura, R. Mizuta, S. Kusonoki, and A. Noda, 2006: Tropical cyclone climatology in a global-warming climate as simukated in a 20 km-mesh global atmospheric model: Frequency and wind intensity analyses. *J. Meteor. Soc. Japan,* **84,** 259–276.

Pielke, R. A. J., and C. W. Landsea, 1999: La Niña, El Niño, and Atlantic hurricane damages in the United States. *Bull. Amer. Meteor. Soc.,* **80,** 2027–2033.

Sabbatelli, T. A., and M. E. Mann, 2007: The influence of climate state variables on Atlantic tropical cyclone occurrence rates. *J. Geophys. Res.,* **112,** D17114, doi:10.1029/2007JD008385.

Santer, S. B., and Coauthors, 2006: Forced and unforced ocean temperature changes in Atlantic and Pacific tropical cyclogenesis regions. *Proc. Natl. Acad. Sci.,* **103,** 13 905–13 910.

Solomon, S., D. Qin, M. Manning, Z. Chen, M. Marquis, K. B. Averyt, M. Tigora, and H. L. Miller, Eds., 2007: *Climate Change 2007: The Physical Science Basis.* Cambridge University Press, 996 pp.

Sugi, M., A. Noda, and N. Sato, 2002: Influence of the global warming on tropical cyclone climatology: An experiment with the JMA global climate model. *J. Meteor. Soc. Japan,* **80,** 249–272.

UNDP/BCPR, 2004: Reducing disaster risk: A challenge for development. United Nations Development Program, Bureau for Crisis Prevention and Recovery, 161 pp. [Available online at www.undp.org/bcpr/disred/rdr.htm.]

Vecchi, G. A., and B. J. Soden, 2007: Increased tropical Atlantic wind shear in model projections of global warming. *Geophys. Res. Lett.,* **34,** L08702, doi:10.1029/2006GL028905.

Vitart, and Coauthors, 2007: Dynamically-based seasonal forecasts of Atlantic tropical storm activity issued in June by EUROSIP. *Geophys. Res. Lett.,* **34,** L16815, doi:10.10292007GL030740.

Webster, P. J., G. J. Holland, J. A. Curry, and H.-R. Chang, 2005: Changes in tropical cyclone number, duration and intensity in a warming environment. *Science,* **309,** 1844–1846.

Yoshimura, J., S. Masato, and A. Noda, 2006: Influence of greenhouse warming on tropical cyclone frequency. *J. Meteor. Soc. Japan,* **84,** 405–428.